

# State-Space Reduction in Deep Q-Networks

Michael Ge\*

Richard Ouyang†

<https://github.com/hahakumquat/stat234-project>

April 24, 2018

## Abstract

Deep convolutional neural networks have become a popular approach to estimating Q-value functions in reinforcement learning problems. These deep Q-networks take in entire images as network inputs, often resulting in large state spaces and long learning times. In this paper, we explore the use of principal component analysis to reduce the state space of image inputs for small network sizes. After testing multiple network configurations, we determine that a reduction in uninformative state features through PCA helps improve the performance of deep reinforcement learning, particularly for small neural network architectures.

---

\*[michaelge@college.harvard.edu](mailto:michaelge@college.harvard.edu)

†[rouyang@college.harvard.edu](mailto:rouyang@college.harvard.edu)

# Contents

<b>1</b>	<b>Introduction</b>	<b>3</b>
<b>2</b>	<b>Background</b>	<b>3</b>
2.1	MDP Overview . . . . .	3
2.2	Deep Q-Networks . . . . .	3
2.3	Principal Component Analysis . . . . .	4
2.4	OpenAI Gym . . . . .	4
2.5	PyTorch . . . . .	5
<b>3</b>	<b>Methods</b>	<b>5</b>
3.1	Initial Setup . . . . .	5
3.2	Image Preprocessing . . . . .	5
3.3	Model Structures . . . . .	5
3.4	Hyperparameters . . . . .	7
3.5	Implementation Details . . . . .	9
<b>4</b>	<b>Results</b>	<b>9</b>
4.1	Random Policy . . . . .	10
4.2	Hyperparameter Tuning Results . . . . .	10
4.2.1	First Grid Search (10,000 Iterations) . . . . .	10
4.2.2	Second Grid Search (50,000 Iterations) . . . . .	12
4.2.3	Third Grid Search (100,000 Iterations) . . . . .	13
4.3	PCA Networks . . . . .	15
4.3.1	Testing Layer Sizes . . . . .	18
4.3.2	Further Testing . . . . .	19
<b>5</b>	<b>Discussion</b>	<b>19</b>
<b>6</b>	<b>Conclusion</b>	<b>22</b>
6.1	Further Directions . . . . .	23
<b>A</b>	<b>Setup Instructions</b>	<b>25</b>

# 1 Introduction

Current methods of Q-learning with deep neural networks are inhibited by the large state space inherent in processing images. The state-of-the-art methods used in recent papers [5, 6, 9] require often infeasible amounts of computational power, time, and data. Although convolutional neural networks theoretically reduce the learning time by restricting the size of the network and accounting for structural information in the data, it is still difficult to learn a good policy in a time- and data-efficient manner. We experiment with reducing the state space dimensionality required by deep Q-networks (DQNs) by applying principal component analysis (PCA) to improve learned policies and training times on a variety of OpenAI games. Although state-space reduction has previously been studied in reinforcement learning [4], use of PCA in reducing state spaces, particularly for neural networks, has not previously been considered.

In addition, we provide an extensible and easy-to-use software framework to test various types of agents and Q-networks, even for games not tested in this paper (such as Atari games).

## 2 Background

### 2.1 MDP Overview

We will briefly describe the general Markov Decision Process (MDP) framework. Define an MDP to be a tuple consisting of the following elements:

- $\mathcal{S}$ , the set of states. In our usage, each state  $s \in \mathcal{S}$  is a transformation of the game screens, which are matrices of pixel values.
- $\mathcal{A}$ , the set of actions. The available actions  $a \in \mathcal{A}$  depend on the setting of the game. In the problems of interest, we consider games with discrete, relatively simple action spaces.
- $r : \mathcal{S} \times \mathcal{A} \rightarrow \mathbb{R}$ , the reward function. A reward  $r_t(s_t, a_t)$  is given to the agent after an action  $a_t$  is taken at state  $s_t$ . The reward is often a complex function. If we knew

the reward function, we would easily know which action to take at any state  $s_t$  and timestep  $t$ .

- $p : \mathcal{S} \times \mathcal{A} \times \mathcal{S} \rightarrow \mathbb{R}$ , the transition probabilities. After taking action  $a$ , the agent moves from state  $s_t$  to state  $s_{t+1}$  with probability  $p(s_{t+1}|s_t, a_t)$ . In our games, transitions are deterministic, so probabilities are either 0 or 1.
- $\gamma \in [0, 1]$ , the discount factor.  $\gamma$  discounts future rewards at a constant, compounded rate.

In reinforcement learning, we seek to learn a policy  $\pi : \mathcal{S} \rightarrow \mathcal{A}$  that maximizes the expected discounted sum of future rewards at a given state:

$$R_t = \mathbb{E} \left[ \sum_{i=t}^{\infty} \gamma^{i-t} r_i | s_{t-1} \right]$$

We define the Q-function under a policy  $\pi$  as the expected discounted sum of future rewards given a state and desired action:

$$Q^\pi(s_t, a_t) = \mathbb{E} [R_t | s_{t-1}, a_{t-1}]$$

The optimal Q-function has been proven to satisfy the Bellman equation:

$$Q^*(s, a) = r(s, a) + \gamma \max_{a' \in \mathcal{A}} Q^*(s', a')$$

### 2.2 Deep Q-Networks

We now briefly discuss the application of deep neural networks to reinforcement learning. The most common use of deep neural networks is to model the Q-function. These deep Q-networks (DQNs) take in a transformed image input  $s$ , passes it through multiple layers, and returns a vector consisting of the estimated  $Q(s, a)$  for all available actions  $a \in \mathcal{A}$ .

Current state-of-the-art models [5, 6] use deep convolutional neural networks (CNNs) as models for the Q-function; these DQNs capitalize on the structure of image data – for example, correlations between nearby pixels – to make Q estimates. Unfortunately, DQNs typically require a

large number of parameters, thus consuming large amounts of computational resources, in terms of both time and space. In our application, due to computational constraints, we restrict our network architectures to contain about 7000 parameters and briefly explore larger parameter spaces toward the end of the paper. More information about the structure of CNNs is available in Figure 1.

Double DQNs (DDQNs) [9] are very similar to regular DQNs. However, instead of using the same network to obtain the target value for mini-batch updates as in a regular DQN, a DDQN randomly selects one of two networks to update and uses the other network to obtain the target value.

### 2.3 Principal Component Analysis

Principal component analysis (PCA) is a dimensionality reduction technique that orthogonally projects the original features into a smaller set of features. PCA chooses the axes with the most variance to construct these principal components. Each of the resulting principal components is uncorrelated with and orthogonal to all the other components. In interpreting images, PCA keeps transformations of the most variable pixels, eliminating the information contained in pixels with very little variance.

We briefly describe how PCA works. Consider a setting where we have  $n$  state feature vectors  $x \in \mathbb{R}^m$ . We construct a feature covariance matrix  $\mathbf{S}$  as the following:

$$\sum_{i=1}^n x_i x_i^\top = \mathbf{X}^\top \mathbf{X} = \mathbf{S}$$

We then consider the  $d$  largest eigenvalues of  $\mathbf{S}$ . It has been shown that the corresponding eigenvectors of these eigenvalues encompass the maximum amount of variance in the dataset in the subspace  $\mathbb{R}^d$ . We then construct a  $d \times m$  projection matrix  $\mathbf{U}$ :

$$\mathbf{U} = (\mathbf{u}_1, \dots, \mathbf{u}_d)^\top$$

For each  $\mathbf{x}$ , we can then compute the transformed feature vector  $\mathbf{z} = \mathbf{U}\mathbf{x}$ . These can also

be interpreted as the reconstruction coefficients.

To reconstruct a simplified version of the original feature vector, we compute:

$$\hat{\mathbf{x}} = \mathbf{U}^\top \mathbf{z}$$

In our usage, we transform our input images into a feature vector of pixels before performing PCA.

### 2.4 OpenAI Gym

OpenAI Gym [2] offers a set of many standard games on which to test reinforcement learning algorithms. We tested our algorithms, which learn on pixel images, on the following games. See Figure 2 for sample images of each game.

**CartPole-v0** `CartPole` is the classic reinforcement learning environment. At every time step, the agent receives a reward of 1 and chooses to push the cart either right or left. The game ends when the pole falls to an angle greater than 15 degrees from vertical or when the cart moves off the screen.

**Acrobot-v1** `Acrobot` is a reinforcement learning game consisting of a double pendulum. The agent can only apply force to the connecting joint (left, right, or no movement) and must swing the pendulum so that the tip of the pendulum reaches a certain height. The agent receives a reward of  $-1$  for every time step the goal is not reached.

**MountainCar-v0** `MountainCar` is a reinforcement learning game in which the agent tries to drive a car up a hill. The car is not strong enough to climb the hill itself and thus must learn to use gravity to achieve the necessary speed. At every time step, the three movements available are accelerating to the right, accelerating to the left, and doing nothing. The agent receives a reward of  $-1$  for every time step the goal is not reached.

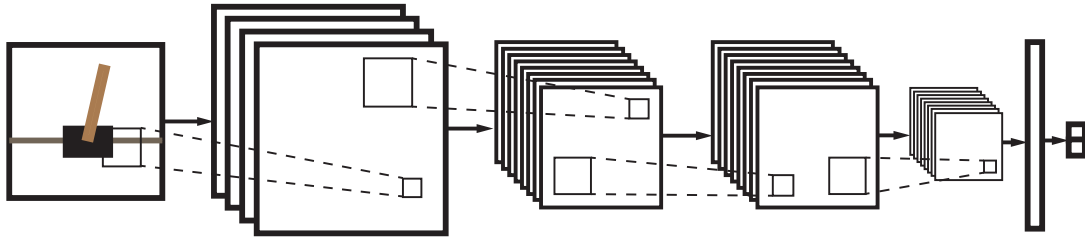


Figure 1: A visualization of the network structure of a convolutional neural network. The input is the image, which is convolved through several layers, each of which contains several filters. The result is then shrunk through a max pooling layer and passed through a fully connected linear layer before being output as Q-values for each action in the action space.

## 2.5 PyTorch

PyTorch [7] is a Python framework for constructing neural network architectures. The language is relatively new and has little online support, so learning the language was a significant part of the project goal. Although PyTorch is still in its early stages of development, it has several advantages compared to other neural network libraries such as TensorFlow and Keras. Namely, improvements include a clean extension of the common Python package NumPy, deep integration with Python, and efficient memory usage.

## 3 Methods

### 3.1 Initial Setup

We replicated the original deep Q-network papers [5, 6] in Python, using PyTorch [7] for the neural network architecture and OpenAI Gym [2] to test and compare our algorithms on different games.

There are quite a few steps to get started to replicate our procedure, including changing some of the source code in OpenAI Gym. For the sake of brevity, these instructions are included in Appendix A. To run our experiments, we used a limited partition of an Odyssey research computing cluster to run a portion of our computationally intensive jobs.

### 3.2 Image Preprocessing

In this project, our goal was to learn the optimal policy for the games without using parametric data – for example, the pole angle in `CartPole`. Instead, we focused more on image processing rather than using the state information given by the Gym environment.

At each time step, we obtained the RGB (color) mapping of the game screen, resized the image to  $80 \times 80$  pixels (rectangular images were squashed into a square), and converted the image to grayscale. We then took the difference between the current timestep’s image and the last timestep’s image as the state to input into our DQN.

### 3.3 Model Structures

In our experiments, we used four different types of models, each of which includes the original (prefixed with “DQ”) and double (prefixed with “DDQ”) network variants:

**(D)DQCNN** The original model [5, 6] and variants [9]. These models convolve images using no extra state-space reduction techniques like PCA. This original, grayscale model is also referred to as the (D)DQN-GS

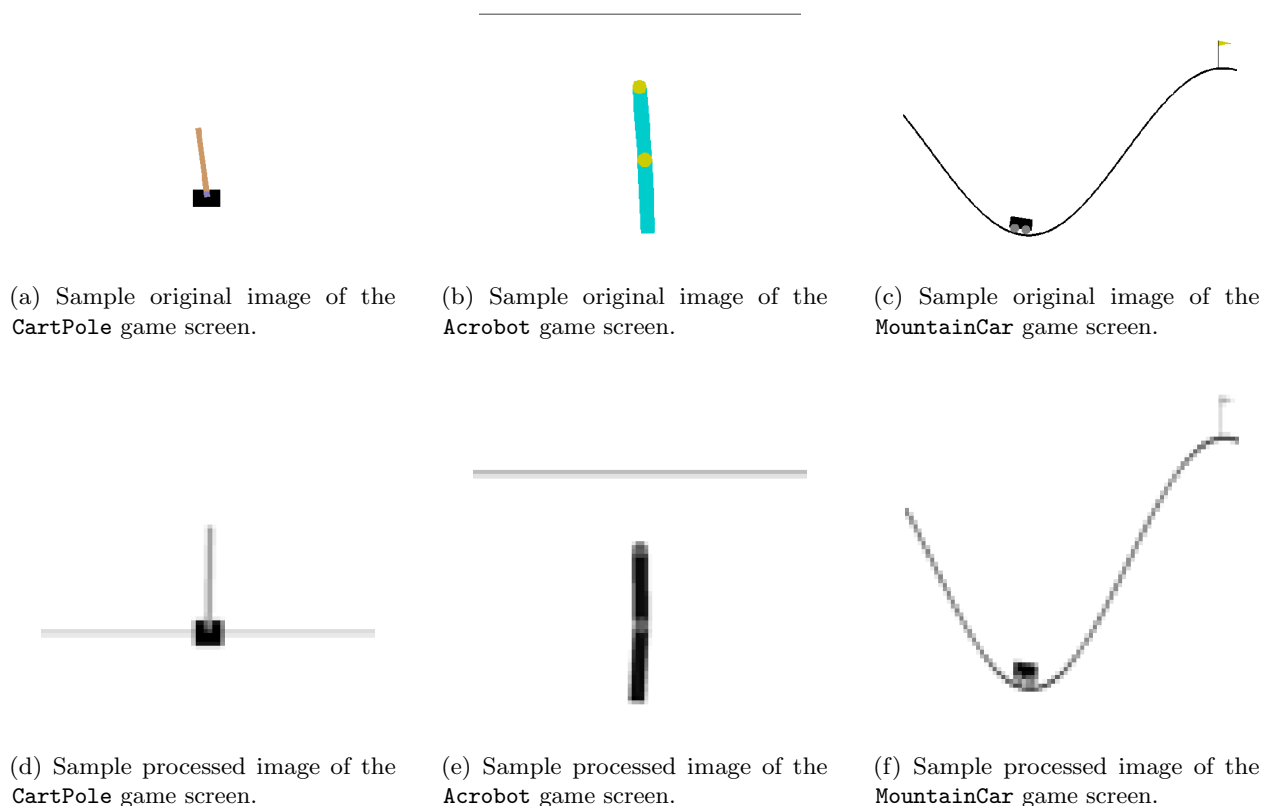


Figure 2: Original and processed images from the three games discussed in this paper. The processed images were created by grayscaling the original images and resizing from  $600 \times 400$  pixels to  $80 \times 80$  pixels. The resulting feature space is then  $\mathbb{R}^{6400}$ .

model. We use these two terms interchangeably.

**(D)DQN-PCA** These models use a database of 1000 states, generated from a random policy, as training data for PCA and project the pixel features of new states onto the subspace that captures at least 99% of the variance. The result for each state is a one-dimensional vector with varying lengths based on the game (100 to 500 features). This vector is passed into a feed-forward (not convolutional) deep neural network with varying numbers of layers and nodes to predict the Q-value.

**(D)DQCNN-PCA** These models also perform PCA; however, the (D)DQCNN-PCA mod-

els then invert the PCA transformation, converting each transformed image back to its original space. The result is a simplified  $80 \times 80$  image, which is then input into a model with the same network structure as the original (D)DQN.

**(D)DQCNN-PCA-Mini** Out of curiosity, we included one additional model type, which takes the one-dimensional vector obtained from the PCA transformation and reshapes it into a square (zero padding if necessary). We then convolved the resulting “image” through a smaller neural network to predict the Q-value for each state. Although PCA strips correlation between nearby pixels, we were interested in investigating whether

the reduced dimensionality preserved some structure between nearby values.

For the (D)DQCNN and (D)DQCNN-PCA models, we kept our network structure similar to [5] and [6] but reduced the parameter size by using three hidden layers in each network. These models take in an  $80 \times 80$  grayscale image. Each hidden layer in the network convolves the previous layer’s output into multiple filters, followed by a batch normalization and a leaky ReLU with  $\alpha = 0.001$  to prevent dead nodes. The first layer convolves  $8 \times 8$  filters with stride 4; the second layer convolves  $16 \times 4 \times 4$  filters with stride 2; the final hidden layer convolves  $16 \times 4 \times 4$  filters, this time with stride 1. A max pooling with kernel size 2 is then applied to reduce the dimensionality of the output. The final layer is fully connected and maps linearly to the number of actions available. For instance, since `CartPole` contains two actions at any time, the output of the neural network contains two nodes. This structure saves time when forwarding through the network, since a single forward pass for a given state  $s$  gives  $\hat{Q}_{\text{network}}(s, a)$  for all  $a \in \mathcal{A}$ . The images can be found in Figure 3.

To ensure that the models are relatively comparable, we kept the number of parameters for each model as close as possible at around 7,000 parameters. For the (D)DQN-PCA model, we tested a variety of network architectures, varying the number of layers as well as the number of nodes in each layer.

For the (D)DQCNN-PCA-Mini model, we kept the rough network structure the same as our original models while accounting for the reduced image size. However, to account for the smaller image size, we reduced the kernel size to 4 and the stride to 1 for all layers.

### 3.4 Hyperparameters

We tested many configurations of hyperparameters, varying the following:

**Model** One of the Q-function models mentioned in Section 3.3.

**Frame skip** The number of time steps for which the same action is repeated. To speed up learning, we used this method described in [5, 6]. When an action is selected, that action is repeated for the next  $k$  frames, since selecting an action and training takes much more time than rendering an additional step of the game. We chose  $k = 3$  since  $k = 4$ , which was suggested in [5, 6], empirically performed worse in `CartPole`.

**Update frequency** The number of distinct action selections between each minibatch update. This value is typically set to 4. This technique speeds up the training even further, since rendering the environment is far less costly than forwarding through the network. This technique has been extensively used in other papers [5, 6, 9].

**Number of training steps** The length of time the model should be trained, expressed in terms of the number of minibatch training steps. While state-of-the-art research uses up to 10 million frames, our resources restrict us to values between 10 thousand and 100 thousand.

**Replay memory size** The maximum number of transitions – each of which is a  $(s, a, r, s')$  tuple – stored in the replay memory. The replay memory is used to reduce correlation between transitions used in each minibatch update [5, 6].

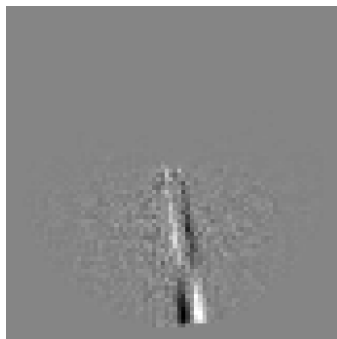
**Target update** If the model uses a target network [6], this represents the number of trains between each target network update. Each update involves setting the target network parameters to the main network parameters.

**Learning rate** The (initial) learning rate used by the optimizer. A higher learning rate results in a model that learns faster but may diverge.

**Learning rate annealing** Whether the learning rate is annealed to a smaller value. Learning rate annealing helps decrease the



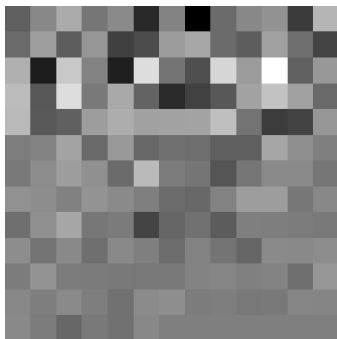
(a) Sample PCA-transformed image of the `CartPole` game screen for the DQCNN-PCA model.



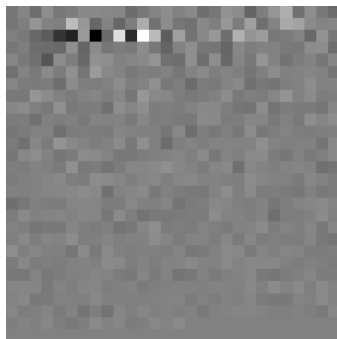
(b) Sample PCA-transformed image of the `Acrobot` game screen for the DQCNN-PCA model.



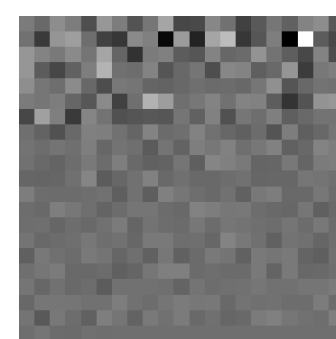
(c) Sample PCA-transformed image of the `MountainCar` game screen for the DQCNN-PCA model.



(d) Sample PCA-transformed image of the `CartPole` game screen for the DQCNN-PCA-Mini model.



(e) Sample PCA-transformed image of the `Acrobot` game screen for the DQCNN-PCA-Mini model.



(f) Sample PCA-transformed image of the `MountainCar` game screen for the DQCNN-PCA-Mini model.

Figure 3: PCA images from the three games discussed in this paper. The PCA images were created by grayscaling the original images, using the features that capture 99% of the variance, and either inverting the transformation or not. The resulting feature space depends on the PCA reduction amount. Note that the most important pixels (near the game object in the first row, and near the top in the second row) are much more variable in color than the less important pixels, which tend to be a relatively uniform gray.

likelihood of policy divergence. The learning rate anneals according to the equation

$$\alpha_t = \alpha_{\text{initial}} \max \left( \exp \left( -\frac{t}{\lambda_\alpha} \right), \frac{0.0005}{\alpha_{\text{initial}}} \right),$$

where  $t$  is the number of minibatch training updates that have already occurred, and  $\lambda$  is the decay rate, so that the learning rate anneals exponentially from its initial value to a final value of 0.0005.

**Batch size** The minibatch size, or the number

of transitions used in each training update. The two values tested were 32 and 128.

**Loss function** The loss function used in the model. The Huber loss (defined as the  $\ell_2$  norm for losses greater than 1 and the  $\ell_1$  norm otherwise) and the mean squared error (MSE) loss were the two loss functions considered.

**Regularization** The weight decay in the optimizer. This value typically ranges from 0 to 1 and is used to prevent overfitting in

our networks.

**Agent action selection** We used an  $\epsilon$ -greedy agent, annealing  $\epsilon$  from  $\epsilon_{\text{initial}} = 1$  to  $\epsilon_{\text{final}} = 0.1$  according to the equation

$$\epsilon_t = \epsilon_{\text{final}} + (\epsilon_{\text{initial}} - \epsilon_{\text{final}}) \exp\left(-\frac{t}{\lambda_\epsilon}\right),$$

where  $t$  is the number of times the agent has already selected an action, and  $\lambda$  is the decay rate.

**Network Architecture** Toward the end of our experimentation, we had the time to test several different network configurations for the (D)DQN-PCA model. Unfortunately, due to the computational demands of performing over images, it was intractable to test larger node structures.

### 3.5 Implementation Details

The code is structured such that the user can pass a model, agent, game, and a large selection of hyperparameters into `main.py`. During the script execution, statistics are logged for later analysis.

Within our `utils/` folder, we implemented several scripts to aid in the data analysis process, some of which we will briefly discuss here.

- `Logger.py` is a general logging utility for storing statistics in files.
- `PCA.py` contains a PCA class whose objects can train on inputs of states, return the transformed features, and invert already-transformed features back into the original image space.
- `ReplayMemory.py` contains a class whose objects store and quickly sample transitions for minibatch updates.
- `get_notes_and_stats.py` parses our raw data into an easy-to-read format, providing summary statistics, hyperparameters, and metadata about each job.

- `plot_data.py` plots raw data as well as running means over episodes and training updates.
- `save_states.py` runs a random policy for each game, saving a large set of states on which PCA can later be performed.

Our `automate_run` folder contains the following bash scripts for running jobs on the computing cluster:

- `gen_slurms.sh` and `search_nets.sh` iterate over a given hyperparameter space and submit batch jobs for each hyperparameter combination in parallel.
- `view_plots.sh` is a utility that allows the user to view the rewards of each game, providing a preliminary categorization of model performance.

Although we did have access to a computing cluster, the access was limited and we did not have access to GPUs, which significantly speed up learning for neural networks. We also had limited time to run our experiments, preventing us from running the 10 million frames per game prescribed in the literature [5, 6]. This was the motivation for our efforts to improve learning by reducing the state space.

## 4 Results

The full set of raw data and metadata are available in our GitHub repository<sup>1</sup> (warning: approximately 600 MB). For all our experiments, our primary measure of policy performance was the mean reward over the second half of the episodes, with a rolling mean over the previous 5% of the total number of episodes providing a similar but smoother representation of model performance. Additionally, all other summary statistics for each run are also taken over the second half of the episodes, after the algorithm has had time to learn the game and converge. This prevents the

<sup>1</sup><https://github.com/hahakumquat/stat234-project/tree/master/data>

learning process from affecting measurements of the final learned policy.

Note that the plots of our data are graphed across all of the episodes completed over a constant number of training iterations rather than over a constant number of episodes. Therefore, the number of episodes varies depending on the durations of each game. That is, for longer game durations, we have fewer episodes. This difference occurs because we seek to keep training time constant between models. For instance, if we were to train models for a constant number of episodes, a poor `MountainCar` model that averages episode durations around 5000 (and thus per-episode rewards around -5000) would be able to use approximately ten times more training time (measured in clock time) than a better `MountainCar` model that averages episode durations around 500 (and thus per-episode rewards around -500). On the other hand, by training models for a constant number of training steps, we ensure that training time as well as the number of minibatch updates is relatively constant between all models. This strategy is consistent with the deep Q-learning literature [5, 6, 9], which typically keeps the number of frames played constant.

For the sake of comparing plots within games, the  $y$ -axes for the reward graphs are standardized, even if episode rewards are outside the axis limits. In particular, the  $y$ -axis is clipped to be between 0 and 200 for `CartPole`,  $-2000$  and 0 for `Acrobot`, and  $-5000$  and 0 for `MountainCar`. We do this because unclipped axes often create difficulties in detecting patterns in regions with low reward variance.

#### 4.1 Random Policy

As a baseline, we ran a random policy on each game, with results in Figures 4, 5, and 6. The average rewards and durations for the three games are available in Table 1. With this initial goal in mind, we proceeded to test different model architectures and hyperparameter settings to achieve good empirical results over all three games.

## 4.2 Hyperparameter Tuning Results

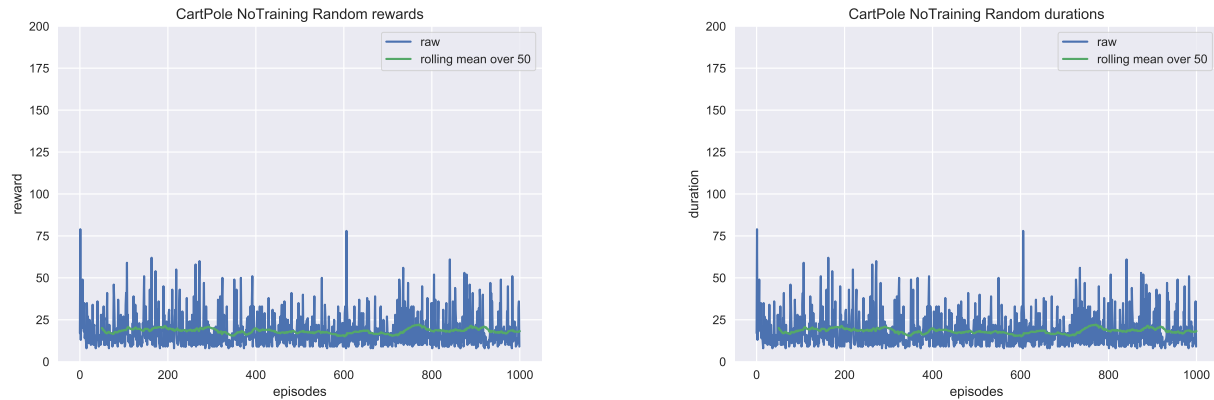
In our hyperparameter tuning, we decided to keep the frame skip, update frequency, replay memory size, and agent action selection hyperparameters constant for testing, since grid search sizes increase exponentially in the number of parameters, and varying these settings would vastly increase simulation time and space consumption.

### 4.2.1 First Grid Search (10,000 Iterations)

In order to establish a solid set of hyperparameters to which PCA variants of DQNs could be compared, we began our experiments with an initial grid search over the hyperparameters of interest for 10,000 training steps to eliminate poorly performing hyperparameter settings. Table 2 contains the results of the top fifteen models for each game ordered by performance.

From these results, we already find that our best hyperparameter configurations beat the random baseline. `MountainCar` was rather difficult to learn, as the final policy seems to depend on the random initialization. With sub-optimal hyperparameters, the episodes under a poorly learned policy can extend to tens of thousands of time steps, far more than a random policy. This particular vulnerability to divergence likely occurs because all transitions entered into the replay memory have  $r = -1$ , creating difficulties in learning. The average episode in `CartPole` roughly doubles the duration of the random policy, though the performance has significantly high variance in all models, reaching maxima of up to 200 time steps. Finally, `Acrobot` seems to have been learned quite quickly, reaching optimal performance within the 10,000 training steps.

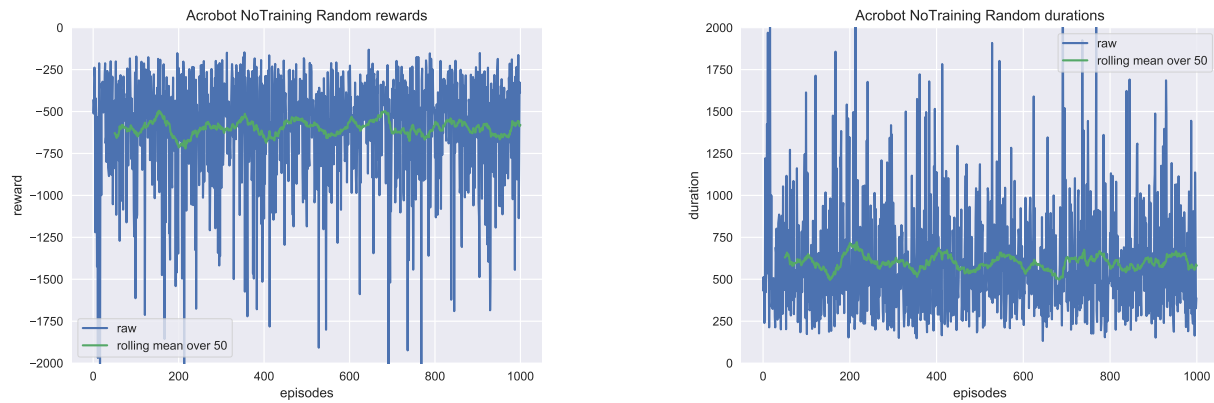
Here, we observe consistently stronger performance by DDQN-GSs relative to DQN-GSs and by using a Huber loss function rather than an MSE loss. Other optimizers, such as Adam, failed to learn in pre-testing, so we used the RMSProp optimizer (as suggested by [5]) throughout our experiments. Weight decay yielded mixed results, likely due to the fact that we only allowed the models to run for 10,000 training steps. Additionally, the effectiveness of the learning rate



(a) Rewards by episode, as well as a rolling mean, for a random policy in the **CartPole** game.

(b) Durations by episode, as well as a rolling mean, for a random policy in the **CartPole** game.

Figure 4: Baseline results from the **CartPole** game from OpenAI Gym under a random policy.



(a) Rewards by episode, as well as a rolling mean, for a random policy in the **Acrobot** game.

(b) Durations by episode, as well as a rolling mean, for a random policy in the **Acrobot** game.

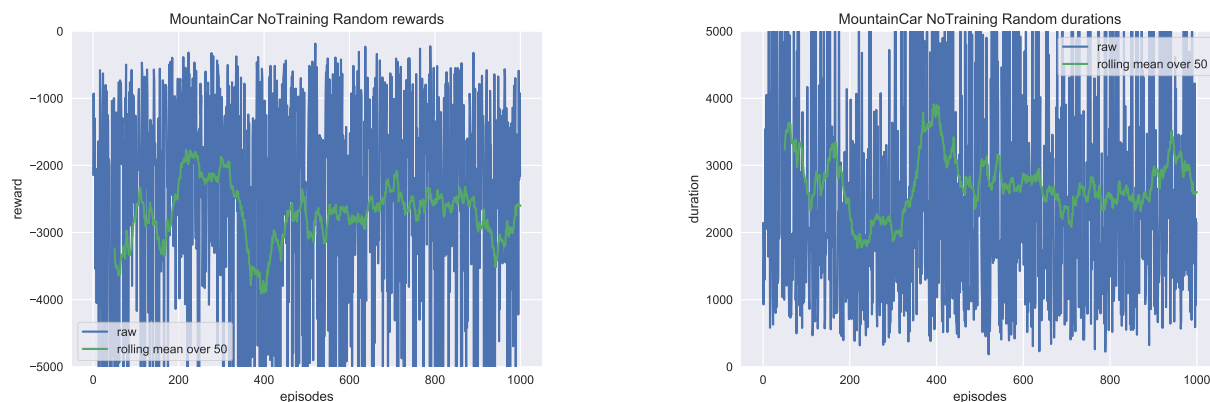
Figure 5: Baseline results from the **Acrobot** game from OpenAI Gym under a random policy.

Game	Average Duration	Average Reward
CartPole-v0	18.441	18.441
Acrobot-v1	599.73	-598.73
MountainCar-v0	2717.77	-2717.77

Table 1: Average rewards and durations under a random policy for the three games.

parameters varied significantly with the game; for example, **CartPole** learns better with a significantly higher learning rate than the other two games. We also saw that annealing the learning rate slightly improved the overall performance of the algorithms, so we decided to keep the an-

nealing for subsequent experiments. In theory, a learning rate annealing should improve the stability of the model after the model has had time to learn a strong policy. Moreover, not displayed in the data is the surprising fact that DQN-GS with an enabled target update performed significantly



(a) Rewards by episode, as well as a rolling mean, for a random policy in the `MountainCar` game.

(b) Durations by episode, as well as a rolling mean, for a random policy in the `MountainCar` game.

Figure 6: Baseline results from the `MountainCar` game from OpenAI Gym under a random policy.

worse than DQN-GSs without a target update in that they failed to reach any convergence at all, so we also decided to remove target update functionality for future experiments. With these observations in mind, we proceeded to test another batch of models using a larger number of training steps.

#### 4.2.2 Second Grid Search (50,000 Iterations)

Setting the optimizer, loss function, and target update to RMSProp, Huber loss, and False, respectively, we performed a second grid search over 50,000 training iterations to tune the learning rate and weight decay. The results can be found in Table 3.

`MountainCar` and `Acrobot` continued to perform well with more training time for the best models, though we began to see evidence of high variance in performance between models for these games. Both had the worst models getting average scores near the level of randomness. In these games, episodes are not completed until the agent succeeds at reaching above a certain height or climbing up the mountain. As a result, if an agent learns a poor policy early on, the agent could spend all of its training iterations receiving  $-1$  reward with no positive feedback. To help mitigate this issue, we capped the number

of training iterations per episode to 20,000 with the intent to expose the agent to more positive states and to speed up learning time. If an agent reaches a duration of 20,000, we already know that the agent does a poor job of learning a good policy and can afford to ignore the model, since in our random policy experiments, episode durations never surpassed 16,000 training steps and rarely lasted more than 10,000 steps.

Again, we see that DDQN-GSs tend to outperform DQN-GSs. The learning rate, however, is inconsistent from the first grid search. Here, we find that overall, lower learning rates are preferred over higher ones for longer grid search durations. This observation is reasonable, since we expect that with a longer training duration, the agent has more time to converge to a good policy, whereas with only 10,000 iterations, the model needs a higher learning rate to quickly outdo random performance. As a result, we decided to continue with even higher training times with lower learning rates. Weight decay does not appear to have a significant impact on the performance of the models, so we decided to take the more conservative option of a regularization coefficient of 0.1.

mean	std	game	model	target	lr	lr_anneal	loss_function	weight_decay
-194.65	40.72	MountainCar-v0	DDQN_GS	N/A	0.0010	False	Huber	0.100
-203.34	51.92	MountainCar-v0	DDQN_GS	N/A	0.0010	False	Huber	0.001
-275.30	143.07	MountainCar-v0	DQN_GS	False	0.0010	False	Huber	0.100
-401.52	174.12	MountainCar-v0	DDQN_GS	N/A	0.0010	False	Huber	0.001
-432.88	184.60	MountainCar-v0	DDQN_GS	N/A	0.0010	False	Huber	0.100
-447.00	188.12	MountainCar-v0	DQN_GS	False	0.0010	False	Huber	0.001
-459.67	203.96	MountainCar-v0	DDQN_GS	N/A	0.0010	True	Huber	0.001
-515.18	260.42	MountainCar-v0	DDQN_GS	N/A	0.0001	True	Huber	0.100
-741.46	475.74	MountainCar-v0	DQN_GS	True	0.0010	False	Huber	0.001
-747.50	485.40	MountainCar-v0	DQN_GS	True	0.0010	False	MSE	0.100
-767.06	544.14	MountainCar-v0	DQN_GS	True	0.0010	False	MSE	0.100
-779.10	593.02	MountainCar-v0	DQN_GS	True	0.0010	True	MSE	0.100
-815.88	514.64	MountainCar-v0	DQN_GS	True	0.0010	False	Huber	0.100
-819.31	400.22	MountainCar-v0	DDQN_GS	N/A	0.0001	True	Huber	0.100
-830.99	585.96	MountainCar-v0	DQN_GS	True	0.0010	True	MSE	0.100
45.09	20.87	CartPole-v0	DDQN_GS	N/A	0.0010	False	Huber	0.100
43.74	18.85	CartPole-v0	DDQN_GS	N/A	0.0010	True	Huber	0.100
42.95	20.65	CartPole-v0	DDQN_GS	N/A	0.0010	False	Huber	0.100
41.33	20.06	CartPole-v0	DDQN_GS	N/A	0.0010	False	Huber	0.001
41.02	17.93	CartPole-v0	DDQN_GS	N/A	0.0001	False	MSE	0.100
38.56	20.58	CartPole-v0	DDQN_GS	N/A	0.0010	True	Huber	0.001
36.85	19.40	CartPole-v0	DDQN_GS	N/A	0.0001	True	Huber	0.001
35.95	20.28	CartPole-v0	DQN_GS	False	0.0001	True	Huber	0.100
34.19	19.59	CartPole-v0	DDQN_GS	N/A	0.0010	False	Huber	0.100
34.05	18.31	CartPole-v0	DDQN_GS	N/A	0.0001	False	Huber	0.100
32.99	18.97	CartPole-v0	DDQN_GS	N/A	0.0010	True	Huber	0.001
32.15	18.75	CartPole-v0	DQN_GS	False	0.0010	False	Huber	0.001
31.80	18.42	CartPole-v0	DDQN_GS	N/A	0.0010	True	Huber	0.001
31.65	18.50	CartPole-v0	DDQN_GS	N/A	0.0010	True	Huber	0.100
31.13	17.34	CartPole-v0	DQN_GS	False	0.0001	False	Huber	0.100
-135.35	40.45	Acrobot-v1	DDQN_GS	N/A	0.0010	False	Huber	0.001
-139.54	48.99	Acrobot-v1	DDQN_GS	N/A	0.0001	True	Huber	0.100
-139.90	68.38	Acrobot-v1	DDQN_GS	N/A	0.0010	False	MSE	0.100
-140.98	47.55	Acrobot-v1	DDQN_GS	N/A	0.0001	True	Huber	0.100
-141.87	47.09	Acrobot-v1	DDQN_GS	N/A	0.0010	False	Huber	0.001
-144.14	49.84	Acrobot-v1	DDQN_GS	N/A	0.0010	True	Huber	0.001
-145.35	55.77	Acrobot-v1	DDQN_GS	N/A	0.0010	False	MSE	0.001
-145.66	56.42	Acrobot-v1	DDQN_GS	N/A	0.0010	True	Huber	0.100
-145.66	67.97	Acrobot-v1	DDQN_GS	N/A	0.0010	False	MSE	0.001
-146.53	51.54	Acrobot-v1	DDQN_GS	N/A	0.0001	True	Huber	0.100
-147.02	57.80	Acrobot-v1	DDQN_GS	N/A	0.0010	False	Huber	0.100
-147.31	47.77	Acrobot-v1	DDQN_GS	N/A	0.0010	False	MSE	0.100
-149.56	52.38	Acrobot-v1	DDQN_GS	N/A	0.0010	True	Huber	0.100
-150.46	48.16	Acrobot-v1	DDQN_GS	N/A	0.0001	True	Huber	0.001
-150.77	90.89	Acrobot-v1	DDQN_GS	N/A	0.0010	False	MSE	0.100

Table 2: Top fifteen parameter-tuned mean rewards per game for our first grid search. Each run used either the DDQN-GS or DQN-GS model and lasted for 10,000 training steps. Note that DDQNs do not have a target update option, so their value in the “target” column is N/A.

#### 4.2.3 Third Grid Search (100,000 Iterations)

By this point, we established that DDQNs tended to outperform DQNs, so we then explored hy-

perparameter configurations that yielded good performance over 100,000 iterations. We then performed a grid search, varying the batch size and learning rate. The results can be found in

mean	std	max	min	game	model	learning_rate	weight_decay
-157.31	43.98	-89.0	-367.0	MountainCar-v0	DDQN_GS	0.001	0.1
-174.80	42.88	-93.0	-367.0	MountainCar-v0	DDQN_GS	0.001	1.0
-183.64	54.77	-86.0	-531.0	MountainCar-v0	DQN_GS	0.010	0.1
-198.51	72.57	-87.0	-692.0	MountainCar-v0	DQN_GS	0.001	0.1
-316.64	99.96	-157.0	-826.0	MountainCar-v0	DDQN_GS	0.001	1.0
-482.91	296.52	-122.0	-2628.0	MountainCar-v0	DDQN_GS	0.001	0.5
-720.04	335.26	-204.0	-3496.0	MountainCar-v0	DDQN_GS	0.010	0.5
-966.51	707.24	-261.0	-8113.0	MountainCar-v0	DDQN_GS	0.010	0.1
-1189.10	895.58	-116.0	-5973.0	MountainCar-v0	DQN_GS	0.001	0.1
-1461.33	1102.82	-187.0	-8273.0	MountainCar-v0	DQN_GS	0.010	0.1
-1540.45	1345.71	-144.0	-9615.0	MountainCar-v0	DQN_GS	0.001	0.5
-1692.36	1668.82	-302.0	-15960.0	MountainCar-v0	DQN_GS	0.010	0.5
-1799.61	1188.13	-152.0	-6791.0	MountainCar-v0	DQN_GS	0.001	1.0
-2137.92	1990.21	-358.0	-14589.0	MountainCar-v0	DDQN_GS	0.010	0.5
-2538.47	2398.58	-124.0	-12525.0	MountainCar-v0	DQN_GS	0.010	0.5
57.91	28.34	277.0	8.0	CartPole-v0	DDQN_GS	0.010	0.5
53.18	26.40	227.0	8.0	CartPole-v0	DDQN_GS	0.010	0.1
53.10	25.76	239.0	8.0	CartPole-v0	DDQN_GS	0.010	1.0
49.23	20.28	178.0	8.0	CartPole-v0	DQN_GS	0.010	0.5
47.78	25.22	208.0	8.0	CartPole-v0	DDQN_GS	0.010	0.5
47.22	25.20	214.0	8.0	CartPole-v0	DDQN_GS	0.010	1.0
46.79	23.67	212.0	8.0	CartPole-v0	DDQN_GS	0.001	0.1
44.75	22.90	216.0	8.0	CartPole-v0	DDQN_GS	0.010	0.1
44.01	20.00	163.0	8.0	CartPole-v0	DQN_GS	0.010	0.5
39.42	23.55	196.0	8.0	CartPole-v0	DDQN_GS	0.001	1.0
38.67	20.16	186.0	8.0	CartPole-v0	DDQN_GS	0.001	1.0
35.83	20.68	198.0	8.0	CartPole-v0	DQN_GS	0.010	0.1
33.11	19.27	152.0	8.0	CartPole-v0	DQN_GS	0.001	0.1
31.10	20.71	166.0	8.0	CartPole-v0	DQN_GS	0.010	0.1
30.34	21.35	175.0	8.0	CartPole-v0	DQN_GS	0.001	0.1
-116.36	29.32	-63.0	-269.0	Acrobot-v1	DDQN_GS	0.010	1.0
-130.94	45.62	-61.0	-608.0	Acrobot-v1	DDQN_GS	0.010	0.1
-142.00	56.06	-64.0	-618.0	Acrobot-v1	DDQN_GS	0.001	1.0
-159.43	78.84	-69.0	-723.0	Acrobot-v1	DDQN_GS	0.001	0.5
-167.35	545.15	-64.0	-20001.0	Acrobot-v1	DDQN_GS	0.001	0.5
-168.79	76.15	-72.0	-821.0	Acrobot-v1	DQN_GS	0.001	0.1
-172.22	113.09	-67.0	-1704.0	Acrobot-v1	DQN_GS	0.001	0.1
-181.91	99.73	-64.0	-1271.0	Acrobot-v1	DDQN_GS	0.010	0.5
-193.88	184.78	-70.0	-3561.0	Acrobot-v1	DDQN_GS	0.001	0.1
-206.12	137.57	-67.0	-3076.0	Acrobot-v1	DQN_GS	0.010	0.1
-210.29	115.62	-75.0	-1161.0	Acrobot-v1	DDQN_GS	0.001	0.1
-222.76	136.54	-67.0	-1443.0	Acrobot-v1	DQN_GS	0.010	0.1
-239.53	340.89	-67.0	-8865.0	Acrobot-v1	DDQN_GS	0.001	1.0
-327.39	270.80	-67.0	-4601.0	Acrobot-v1	DDQN_GS	0.010	0.5
-469.47	1114.24	-102.0	-19928.0	Acrobot-v1	DDQN_GS	0.010	1.0

Table 3: Top fifteen parameter-tuned mean rewards per game for our second grid search. All experiments used a Huber loss, learning rate annealing, no target update, and the RMSProp optimizer for 50,000 training steps.

Table 4.

The data here indicate mixed results. **MountainCar** tends to do better with larger batch sizes, while **Acrobot** and **CartPole** do better

with a smaller batch size. The learning rates differed from game to game as well. With no significant trends in performance, we opted to use a batch size of 128 to increase learning speed

mean	std	max	min	game	batch_size	lr
-220.09	56.98	-109.0	-750.0	MountainCar-v0	128	0.010
-223.76	59.65	-115.0	-731.0	MountainCar-v0	128	0.001
-229.75	65.07	-111.0	-714.0	MountainCar-v0	128	0.005
-257.19	111.89	-92.0	-1510.0	MountainCar-v0	32	0.001
-342.39	128.86	-159.0	-1044.0	MountainCar-v0	32	0.005
-882.25	601.97	-149.0	-4762.0	MountainCar-v0	32	0.010
-8222.00	1780.00	-6442.0	-10002.0	MountainCar-v0	32	0.001
-10002.00	0.00	-10002.0	-10002.0	MountainCar-v0	128	0.001
51.25	27.66	271.0	8.0	CartPole-v0	32	0.010
50.47	25.31	250.0	8.0	CartPole-v0	128	0.001
49.22	24.09	230.0	8.0	CartPole-v0	32	0.001
46.82	24.16	247.0	8.0	CartPole-v0	32	0.005
34.33	18.06	107.0	8.0	CartPole-v0	128	0.001
10.19	2.89	38.0	8.0	CartPole-v0	32	0.001
9.86	2.21	75.0	8.0	CartPole-v0	128	0.005
9.72	1.82	46.0	8.0	CartPole-v0	128	0.010
-116.24	34.05	-63.0	-436.0	Acrobot-v1	32	0.005
-163.57	67.57	-64.0	-987.0	Acrobot-v1	32	0.001
-172.75	66.27	-70.0	-658.0	Acrobot-v1	32	0.010
-227.93	93.22	-103.0	-516.0	Acrobot-v1	128	0.001
-408.08	262.05	-137.0	-1184.0	Acrobot-v1	32	0.001
-453.32	259.88	-97.0	-2454.0	Acrobot-v1	128	0.010
-546.15	631.72	-69.0	-10002.0	Acrobot-v1	128	0.001
-721.18	430.19	-127.0	-3440.0	Acrobot-v1	128	0.005

Table 4: Complete results for our third grid search, sorted by mean reward. All experiments used the DDQN-GS model with a Huber loss function, learning rate annealing, and a 0.1 weight decay for 100,000 training iterations.

and a learning rate of 0.001 to prevent divergence. Our final hyperparameters, used in the rest of the paper, are available in Table 5.

### 4.3 PCA Networks

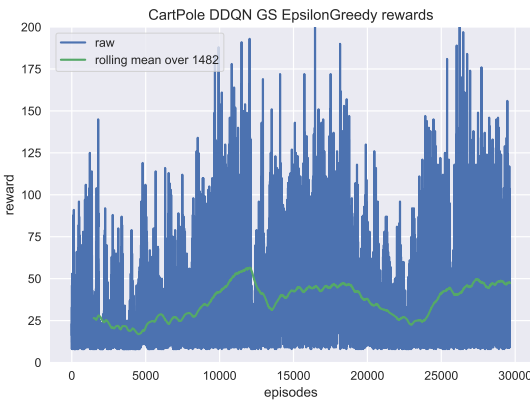
The hyperparameter comparison results generalized quite well to other models, so we continued to use these parameters for all models in the remaining experiments. With a strong DDQN-GS model selected as our new baseline, we then began to test the performance of PCA-based models. With `MountainCar` and `Acrobot` being solved problems for several of our neural networks but `CartPole` failing to ever reach particularly large scores, we then focused our efforts on improving `CartPole`. We then ran a set of experiments for 100,000 iterations over all of our models. See Figures 7, 8, and 9 for a graphical comparison between the double versions of all of the networks of interest. Table 6 contains the full numerical set of results.

First, we note that the (D)DQN-PCA model, which does not convolve over an image representation, does relatively poorly in all settings. This result is surprising; despite the fact that this model does not account for the structural properties of adjacent pixels as a convolutional neural network does, the model performs only slightly better than random. This became a sign that the neural network architecture selected for these models were underfitting the data. For now, we turn our attention to the convolutional PCA versions of the models.

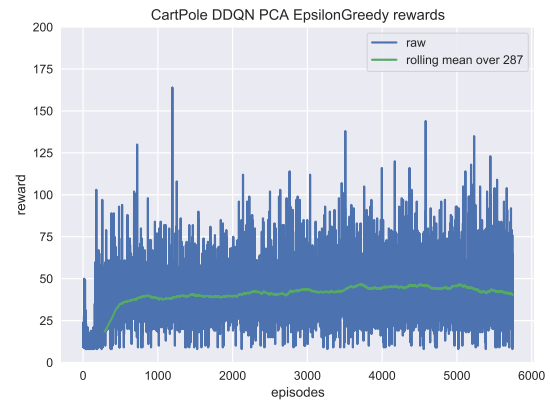
The DDQCNN-PCA model performed well for `CartPole` and `Acrobot`, outperforming even the convolutional models and generating some of the best scores and most stable means we ever saw in our experiments. One possible reason for the superior performance is the fact that PCA simplifies the images, thereby reducing noise and allowing for more efficient learning. Unfortunately, these results were not replicated in the Moun-

Hyperparameter	Value
Model	DDQN
Frame skip	3
Update frequency	4
Training updates	100000
Replay memory size	10000
Target update	N/A
Learning rate	0.001
Learning rate annealing	Yes
Batch size	128
Loss function	Huber loss
Regularization	0.1

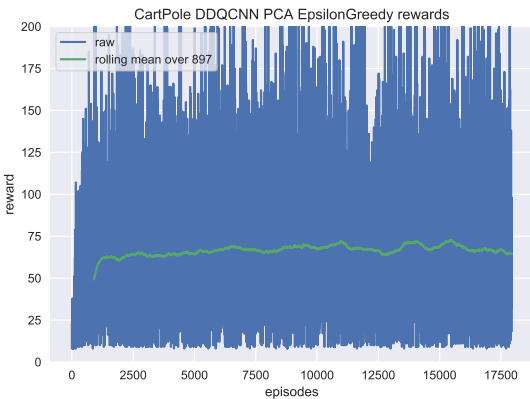
Table 5: The hyperparameters found by our grid search and used for the PCA variants of the (D)DQN, in Section 4.3.



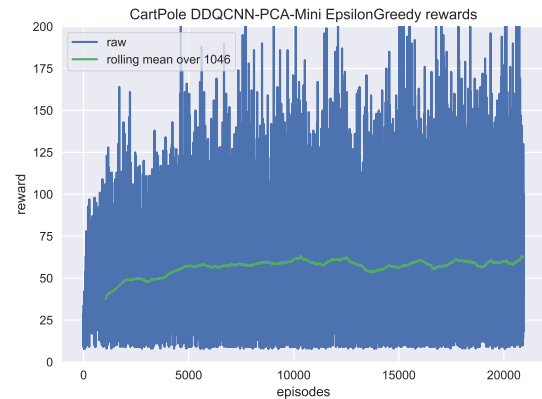
(a) Rewards by episode from training the DDQN-GS model on the **CartPole** game.



(b) Rewards by episode from training the DDQN-PCA model on the **CartPole** game.

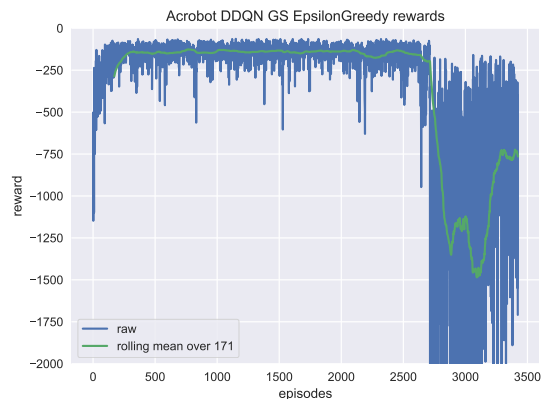


(c) Rewards by episode from training the DDQCNN-PCA model on the **CartPole** game.

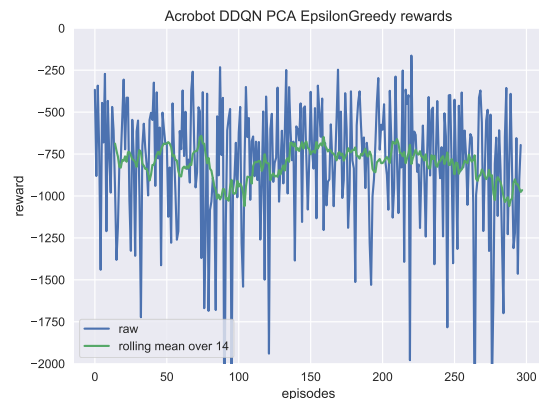


(d) Rewards by episode from training the DDQCNN-PCA-Mini model on the **CartPole** game.

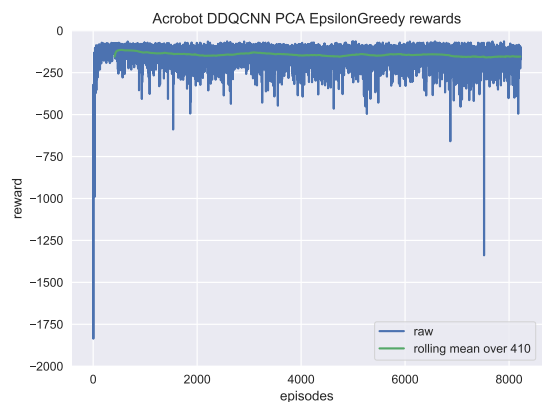
Figure 7: Rewards by episode for four DQN variants (including those using PCA) on the **CartPole** game. All trials used the hyperparameters detailed in Figure 5.



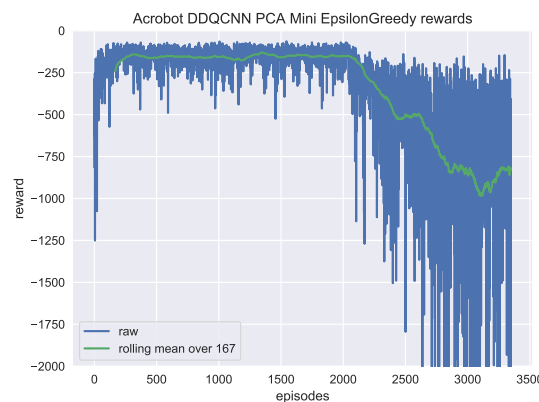
(a) Rewards by episode from training the DDQN-GS model on the Acrobot game.



(b) Rewards by episode from training the DDQN-PCA model on the Acrobot game.



(c) Rewards by episode from training the DDQCNN-PCA model on the Acrobot game.



(d) Rewards by episode from training the DDQCNN-PCA-Mini model on the Acrobot game.

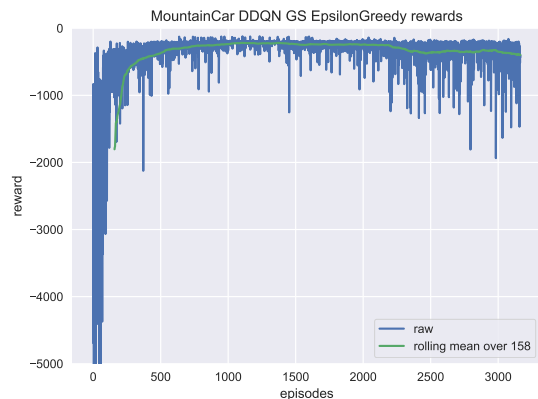
Figure 8: Rewards by episode for four DQN variants (including those using PCA) on the Acrobot game. All trials used the hyperparameters detailed in Figure 5.

`tainCar` game, failing to beat even the random baseline. It seems that `MountainCar` is sensitive to weight initialization, causing unpredictable fluctuations in its performance.

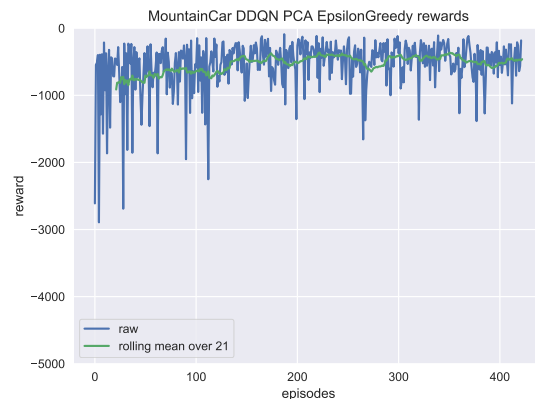
What is more surprising is the performance of DDQCNN-PCA-Mini model, which was a strong performer in the `MountainCar` setting. We had no expectations that this model would do well. After all, the PCA simply selects the most variable features in the projected subspace and are *ad hoc* formed into a square image over which to convolve without maintaining the structural integrity of the original image. It may be that the projection yielded features in the reduced space that had high correlation between one another

and thus high predictive power, which the DQN was able to detect; another possibility is the fact that the orthogonal projection preserved some structural information. Otherwise, we have little explanation for the model’s performance and mention it only as a point of interest for future work.

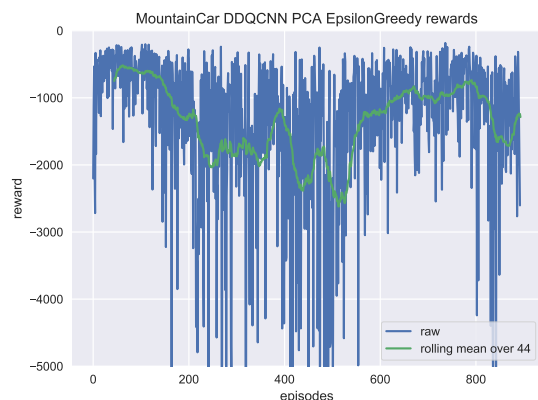
Despite some PCA variants being high performers in each of the games, many of the remaining PCA models were unable to perform above a random baseline, particularly those not using convolutional neural networks. Upon closer inspection of the reward graphs, we find that several PCA models reached a strong optimum around the middle of the training process but



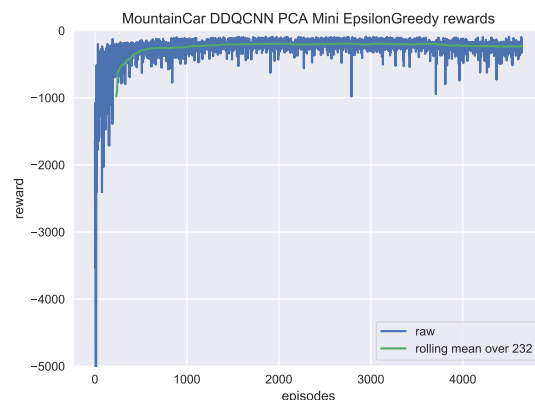
(a) Rewards by episode from training the DDQN-GS model on the `MountainCar` game.



(b) Rewards by episode from training the DDQN-PCA model on the `MountainCar` game.



(c) Rewards by episode from training the DDQCNN-PCA model on the `MountainCar` game.



(d) Rewards by episode from training the DDQCNN-PCA-Mini model on the `MountainCar` game.

Figure 9: Rewards by episode for four DQN variants (including those using PCA) on the `MountainCar` game. All trials used the hyperparameters detailed in Figure 5.

ended up diverging over time. Overall, we find that PCA is sensitive to divergence for bad parameter settings, but less so than the original model; additionally, under the right use cases, the right learning rate annealing, and  $\epsilon$  decay, PCA is a promising method to increase the performance of a Q-network under short learning time settings.

### 4.3.1 Testing Layer Sizes

Due to limited time and resources, one regret we had was that we were unable to tune network configurations throughout the process. However, after seeing our initial set of results, we had suspi-

cions that the models were underfitting the problems of interest. Seeing that the (D)DQN-PCA models performed surprisingly poorly, we decided to test these models on a variety of more complex feed-forward network architectures used in these models. See Table 7 for the results from testing several feed-forward deep neural network architectures for the DDQN-PCA model over 20,000 training iterations.

These findings show a significant increase in the performance of both models, despite losing the structural correlations between pixels. It seems that our initial (D)DQN-PCA neural network architecture was indeed underfitting the images. By adding more weights, (initially 7,000

mean	std	max	min	game	model
-193.61	66.17	-94.0	-816.0	MountainCar-v0	DQN_GS
-210.73	69.85	-88.0	-981.0	MountainCar-v0	DDQCNN_PCA_Mini
-314.35	180.27	-123.0	-1936.0	MountainCar-v0	DDQN_GS
-611.61	419.63	-91.0	-3554.0	MountainCar-v0	DQCNN_PCA
-650.51	456.30	-110.0	-3208.0	MountainCar-v0	DQN_PCA
-1309.16	1106.23	-182.0	-10002.0	MountainCar-v0	DDQCNN_PCA
-1792.34	1358.56	-231.0	-9085.0	MountainCar-v0	DQCNN_PCA_Mini
67.93	36.91	314.0	8.0	CartPole-v0	DDQCNN_PCA
65.26	34.13	350.0	8.0	CartPole-v0	DQCNN_PCA
46.96	23.44	193.0	8.0	CartPole-v0	DQCNN_PCA_Mini
39.80	24.49	243.0	8.0	CartPole-v0	DDQN_GS
29.12	18.95	153.0	8.0	CartPole-v0	DQN_GS
23.99	15.83	142.0	8.0	CartPole-v0	DQN_PCA
11.65	5.32	73.0	8.0	CartPole-v0	DDQCNN_PCA_Mini
-148.55	56.72	-63.0	-1339.0	Acrobot-v1	DDQCNN_PCA
-182.30	116.44	-71.0	-2133.0	Acrobot-v1	DQN_GS
-542.64	803.36	-64.0	-10002.0	Acrobot-v1	DDQN_GS
-550.60	522.97	-69.0	-7599.0	Acrobot-v1	DDQCNN_PCA_Mini
-863.38	413.66	-202.0	-3397.0	Acrobot-v1	DQCNN_PCA_Mini
-868.68	429.20	-113.0	-2913.0	Acrobot-v1	DQCNN_PCA
-1654.28	893.27	-366.0	-5749.0	Acrobot-v1	DQN_PCA

Table 6: Model comparison with final hyperparameters over 100,000 training iterations.

parameters but now over 20,000), we were able to see strong performances from these previously underperforming models.

With these results, we chose the best overall neural network architecture, a two-layer model containing 128 nodes in the first hidden layer and 64 nodes in the second hidden layer. Comparing its results to the rest of the neural networks, we do find a significant increase in the performance. Note that we were unfortunately unable to try larger network configurations on the convolutional models. Being the case that we were unable to even run many of the simulations locally, we decided that if the simulations could not run on our own machines, they would not be fair agents to play the games anyway.

### 4.3.2 Further Testing

With our new DDQN-PCA model, we decided to compare its performance over a longer training time to the original model. Indeed, we continue to see much better performance from our PCA model, even compared to our best previous model, although at the cost of a much slower convergence. For instance, in `CartPole`, the mean

reward reached more than 80, which is nearly 20 more than our previous best model; additionally, the maximum reward we saw was 408, more than 50 higher than our previous maximum. Full results are available in Figure 10 and Table 8.

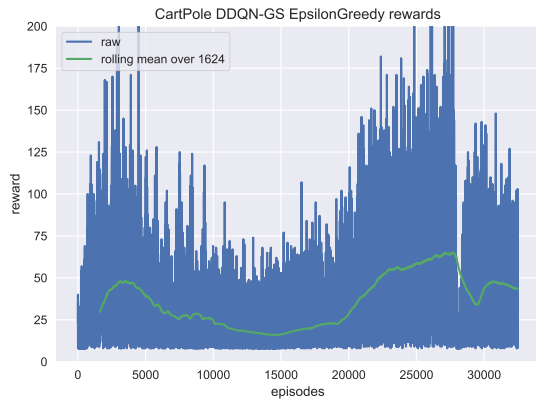
## 5 Discussion

Throughout this exploratory project, we found that learning to play games from image data alone makes each problem significantly harder. While we had the option to read in metadata about each state such as the pole’s angle, the cart’s location, or the car’s velocity, we decided that the best way to standardize the performance of our model was to ensure that each game fed in only pixels. Note that there are many simulations online that claim to learn better scores for `CartPole` even just by using pixel data, but these simulations take advantage of knowing the cart location and cropping the whitespace around the cart, drastically improving the performance of the convolution. On the other hand, we sought to learn the games without any prior knowledge whatsoever.

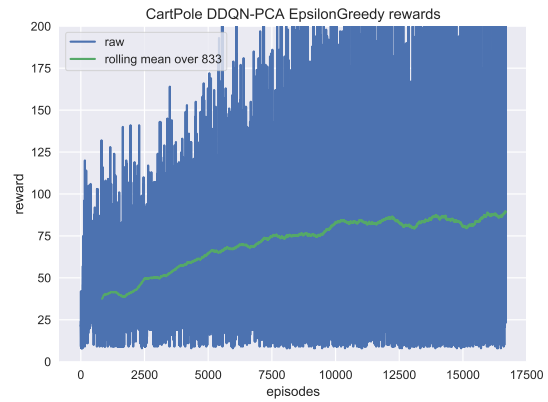
mean	std	max	min	game	model	layer_sizes
-202.72	52.17	-89.0	-431.0	MountainCar-v0	DDQN-PCA	[128]
-330.57	99.83	-159.0	-923.0	MountainCar-v0	DDQN-PCA	[64]
-337.95	139.88	-159.0	-1629.0	MountainCar-v0	DDQN-PCA	[32]
-386.76	253.57	-106.0	-1574.0	MountainCar-v0	DDQN-PCA	[128-128-64-32]
-392.24	168.77	-122.0	-1123.0	MountainCar-v0	DDQN-PCA	[64-32]
-393.12	161.26	-117.0	-944.0	MountainCar-v0	DDQN-PCA	[32-32]
-400.07	189.48	-107.0	-1209.0	MountainCar-v0	DDQN-PCA	[64-64]
-401.32	183.10	-148.0	-1366.0	MountainCar-v0	DDQN-PCA	[128-64]
-405.84	123.67	-204.0	-831.0	MountainCar-v0	DDQN-PCA	[16]
-498.66	237.75	-162.0	-1573.0	MountainCar-v0	DDQN-PCA	[32-16]
-498.93	297.34	-119.0	-1767.0	MountainCar-v0	DDQN-PCA	[128-64-32]
-518.32	273.43	-127.0	-1504.0	MountainCar-v0	DDQN-PCA	[64-16]
-571.04	343.37	-140.0	-2108.0	MountainCar-v0	DQN-PCA	[32-32]
-584.62	347.47	-131.0	-2104.0	MountainCar-v0	DDQN-PCA	[64-32-16]
-586.17	362.75	-118.0	-2239.0	MountainCar-v0	DQN-PCA	[128-64]
63.71	26.29	202.0	8.0	CartPole-v0	DDQN-PCA	[128-128-64-32]
57.89	24.10	187.0	8.0	CartPole-v0	DDQN-PCA	[128-64-32]
52.73	24.69	155.0	8.0	CartPole-v0	DDQN-PCA	[128-64]
50.33	22.70	192.0	8.0	CartPole-v0	DDQN-PCA	[64-64]
50.31	21.42	145.0	8.0	CartPole-v0	DDQN-PCA	[64-32-16]
46.99	22.09	200.0	8.0	CartPole-v0	DDQN-PCA	[128]
46.29	18.98	155.0	8.0	CartPole-v0	DDQN-PCA	[64-32]
45.38	21.62	157.0	8.0	CartPole-v0	DDQN-PCA	[64-16]
44.77	19.33	151.0	9.0	CartPole-v0	DDQN-PCA	[16-32-64]
43.82	21.18	173.0	8.0	CartPole-v0	DDQN-PCA	[16-32]
43.11	18.27	159.0	8.0	CartPole-v0	DDQN-PCA	[32-32-16]
42.28	21.60	157.0	8.0	CartPole-v0	DDQN-PCA	[64]
39.52	19.67	137.0	8.0	CartPole-v0	DDQN-PCA	[32]
38.42	16.44	142.0	8.0	CartPole-v0	DDQN-PCA	[16]
38.31	19.40	141.0	8.0	CartPole-v0	DDQN-PCA	[32-32]
-152.06	74.84	-69.0	-639.0	Acrobot-v1	DDQN-PCA	[128-64]
-197.20	80.54	-81.0	-627.0	Acrobot-v1	DDQN-PCA	[128]
-255.91	127.49	-94.0	-804.0	Acrobot-v1	DDQN-PCA	[64]
-320.71	172.92	-101.0	-1504.0	Acrobot-v1	DDQN-PCA	[64-16]
-457.60	239.31	-148.0	-1618.0	Acrobot-v1	DDQN-PCA	[32]
-561.87	296.20	-139.0	-1731.0	Acrobot-v1	DDQN-PCA	[64-32]
-585.08	265.25	-160.0	-1489.0	Acrobot-v1	DDQN-PCA	[32-16]
-613.99	310.42	-163.0	-2200.0	Acrobot-v1	DDQN-PCA	[32-32-16]
-639.41	303.16	-171.0	-2040.0	Acrobot-v1	DDQN-PCA	[64-64]
-668.13	332.37	-144.0	-2084.0	Acrobot-v1	DDQN-PCA	[64-32-16]
-695.74	323.70	-155.0	-1838.0	Acrobot-v1	DQN-PCA	[64]
-704.81	372.62	-238.0	-2906.0	Acrobot-v1	DQN-PCA	[16]
-708.33	353.32	-189.0	-2049.0	Acrobot-v1	DDQN-PCA	[16]
-735.68	356.00	-259.0	-2472.0	Acrobot-v1	DQN-PCA	[16-32-64]
-763.06	340.41	-123.0	-1670.0	Acrobot-v1	DDQN-PCA	[128-128-64-32]

Table 7: Results from testing several feed-forward deep neural network architectures for the DDQN-PCA model, sorted by reward in descending order. Only the top fifteen results from each game are shown. All experiments used a Huber loss function, learning rate annealing, a batch size of 128, a learning rate of 0.001, and a 0.1 weight decay for 20,000 training iterations.

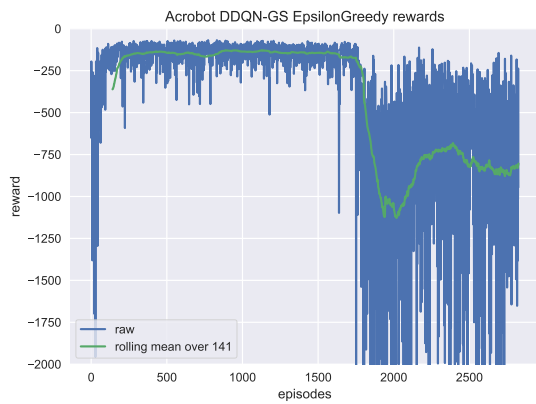
One thing not discussed in great detail was how we decided upon which parameters we chose at every step. In addition to empirical evaluations, we also built generalized linear models on our hyperparameters, treating them as categorical variables and regressing on the mean.



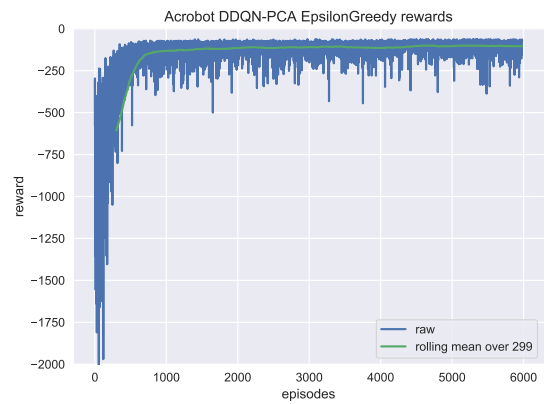
(a) Rewards by episode from training the DDQN-GS model on the **CartPole** game.



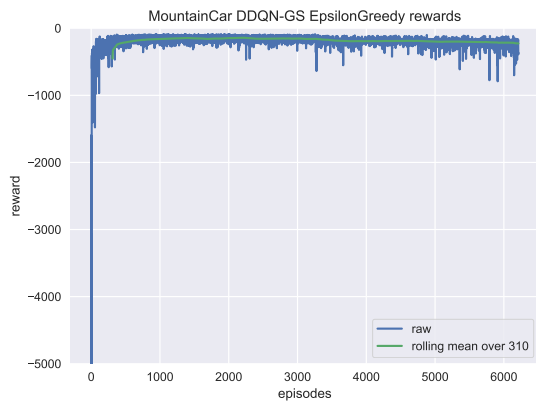
(b) Rewards by episode from training the DDQN-PCA model on the **CartPole** game.



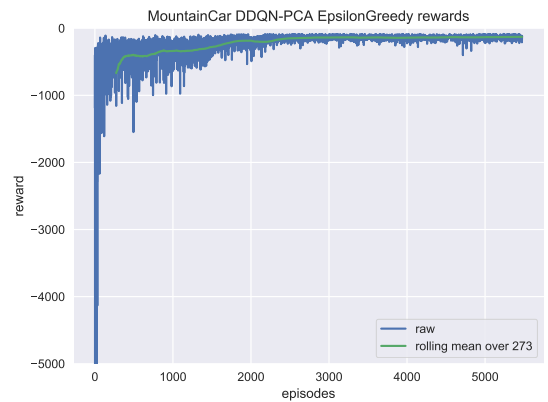
(c) Rewards by episode from training the DDQN-GS model on the **Acrobot** game.



(d) Rewards by episode from training the DDQN-PCA model on the **Acrobot** game.



(e) Rewards by episode from training the DDQN-GS model on the **MountainCar** game.



(f) Rewards by episode from training the DDQN-PCA model on the **MountainCar** game.

Figure 10: Rewards by episode for two DQN variants for all three games. All trials used the hyperparameters detailed in Figure 5.

mean	std	max	min	game	model
-135.79	29.42	-84.0	-401.0	MountainCar-v0	DDQN-PCA
-176.94	63.44	-86.0	-1259.0	MountainCar-v0	DQN-GS
-197.65	53.98	-88.0	-791.0	MountainCar-v0	DDQN-GS
-660.19	471.74	-102.0	-3688.0	MountainCar-v0	DQN-PCA
83.34	49.25	408.0	8.0	CartPole-v0	DDQN-PCA
44.76	26.82	229.0	8.0	CartPole-v0	DDQN-GS
31.59	21.88	234.0	8.0	CartPole-v0	DQN-GS
29.56	16.25	167.0	8.0	CartPole-v0	DQN-PCA
-106.09	37.88	-63.0	-445.0	Acrobot-v1	DDQN-PCA
-218.67	155.54	-66.0	-2227.0	Acrobot-v1	DQN-GS
-681.62	629.47	-74.0	-10002.0	Acrobot-v1	DDQN-GS
-2353.20	1410.17	-281.0	-10002.0	Acrobot-v1	DQN-PCA

Table 8: Comparison between our (D)DQN-PCA models and the literature’s convolutional models using our final hyperparameters (see Table 5) over 100,000 training iterations.

By examining the coefficients of the model, this gave us a rough estimate of how different features were correlated with the mean reward of each model. The results were consistent with our own observations of the performances of specific hyperparameters.

An interesting problem that we encountered while testing different models was that there was little correlation between the loss function and the performance of the model. Indeed, more often than not, the loss function hovered around the same value, typically less than 0.1, as the simulations ran without ever converging toward an actual minimization. Typically, this indicates that we are underfitting our model, since the model is never able to minimize the loss; however, online discussions claim that this is not a problem in a reinforcement learning setting [3].

To see a less noisy version of the per-episode reward, we also kept track of changes in Q-values as the model trained. We randomly sampled a set of 128 states from the replay memory and determined the average Q-value over all states after each episode. Over time, we expect the sample states’ Q-values to increase as the policy improves and the expected future return increases. Indeed, the Q-values for the sample states do tend to increase as the policy learns. Notably, for games with negative rewards (**Acrobot** and **MountainCar**), the sample Q-value starts around 0 and decreases sharply at the very beginning of the training before increasing slightly as the policy

converges. This phenomenon is expected and is an artifact of the fact that the model initially does not yet know that typical episodes have negative rewards. Additionally, because the sample Q-values are determined using the maximum Q-value over all actions, which tends to be an overestimate, the Q-values tend to be overestimates of the empirical rewards for all games. Additionally, this observation is consistent with the fact that the action is selected using the Q-value for the optimal policy, which tends to be better than the  $\epsilon$ -greedy policy’s occasional random action selection. See Figure 11 for an example Q-value plot.

## 6 Conclusion

To conclude, we have built up a robust coding framework to test different Q-function models on a variety of discrete-space OpenAI games. The results suggest that compared to the original model, the de-noising and state-space reduction provided by PCA helps PCA-based variants of DQNs perform quite well in several games. However, these variants do not do as well in games with exceptionally long durations and sparse rewards. With the right model regularization and network architecture, PCA is a promising way to increase model performance for reinforcement learning by reducing the state space and eliminating the need for DQNs to learn unimportant feature information.

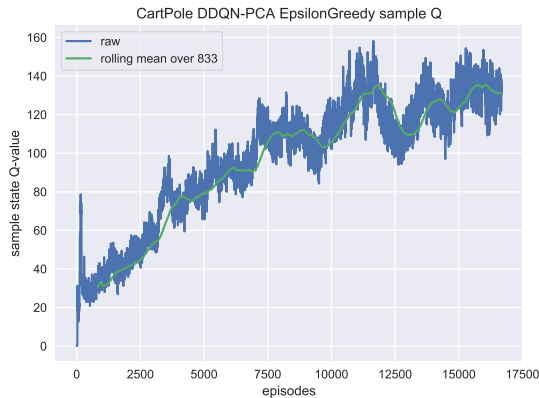


Figure 11: An example plot of the average optimal Q-value over 128 randomly chosen states. This particular graph is for our best model, a DDQN-PCA with two hidden layers of sizes 128 and 64, trained for 100,000 minibatch updates. Note the steady increase in average optimal Q-value as the policy improves.

## 6.1 Further Directions

The obvious next step would be to test the convolutional models using different and larger network configurations to see whether PCA continues to provide improvements. Given our findings, because CNNs capture structural information, we expect that convolutions will improve enough to do better than the DDQN-PCA model tested at the end of this paper and will be further improved by PCA denoising or dimensionality reduction.

Other promising directions include performing the same PCA analysis for DQN performance on other games, particularly Atari games. Games with large (but discrete) action spaces are also good candidates, since the games used in our experiments had only two or three actions. Additionally, extensions to games with continuous action spaces, which would likely need a significantly different network architecture (such as a convolutional neural network linked with a network in which actions are the inputs), pose an interesting problem for DQNs, whose network structure relies heavily on the presence of a discrete action space.

We had severely limited computational power and time, so extending this work using more var-

ied learning rates and annealing schedules could offer better performance. Also, computing using GPUs (which were unfortunately not available) rather than CPUs would have been a substantial time boost.

Recent developments and additions to DQNs also suggest promising improvements to the general DQN framework as well as the use of PCA in reinforcement learning. For instance, adding hindsight experience replay [1] or prioritized experience replay [8], particularly to *MountainCar*, which is heavily dependent on choosing the right transitions in each minibatch update, would further improve our algorithms' performance and check the robustness of using PCA with slightly different learning algorithms.

## References

- [1] Marcin Andrychowicz, Filip Wolski, Alex Ray, Jonas Schneider, Rachel Fong, Peter Welinder, Bob McGrew, Josh Tobin, Pieter Abbeel, and Wojciech Zaremba. Hindsight experience replay. In *Advances in Neural Information Processing Systems*, pages 5048–5058, 2017.
- [2] Greg Brockman, Vicki Cheung, Ludwig Pettersson, Jonas Schneider, John Schulman, Jie Tang, and Wojciech Zaremba. OpenAI Gym, 2016.
- [3] [shimao](#). Loss not decreasing but performance is improving. Cross Validated. <https://stats.stackexchange.com/q/313881> (version: 2017-11-15).
- [4] Yasutaka Kishima and Kentarou Kurashige. Reduction of state space in reinforcement learning by sensor selection. *Artificial Life and Robotics*, 18(1-2):7–14, 2013.
- [5] Volodymyr Mnih, Koray Kavukcuoglu, David Silver, Alex Graves, Ioannis Antonoglou, Daan Wierstra, and Martin Riedmiller. Playing Atari with deep reinforcement learning. *arXiv preprint arXiv:1312.5602*, 2013.
- [6] Volodymyr Mnih, Koray Kavukcuoglu, David Silver, Andrei A Rusu, Joel Veness, Marc G Bellemare, Alex Graves, Martin Riedmiller, Andreas K Fidjeland, Georg Ostrovski, et al. Human-level control through deep reinforcement learning. *Nature*, 518(7540):529, 2015.
- [7] Adam Paszke, Sam Gross, Soumith Chintala, and Gregory Chanan. PyTorch, 2017.
- [8] Tom Schaul, John Quan, Ioannis Antonoglou, and David Silver. Prioritized experience replay. *arXiv preprint arXiv:1511.05952*, 2015.
- [9] Hado Van Hasselt, Arthur Guez, and David Silver. Deep reinforcement learning with double Q-learning. In *AAAI*, volume 16, pages 2094–2100, 2016.

## A Setup Instructions

1. Download/install Anaconda
2. Clone this paper's repository: <https://github.com/hahakumquat/stat234-project>
3. Inside the directory containing the repository, create and activate the `conda` environment, which consists of all the necessary packages:

```
conda env create -f environment.yml
source activate stat234
```

4. Fix errors if unmerged into master OpenAI Gym branch
  - Consistent with the pull request at <https://github.com/openai/gym/pull/972>, in each of the game files in `gym/gym/envs/classic_control/`, add `dtype=np.float32` to each `spaces.Box()` initialization to suppress the logger warning
5. Run `main.py`
  - `python main.py -h` for command-line argument instructions and a full list of arguments and defaults.
  - `python main.py -g CartPole-v0 -m DQN_GS -e 1000` for training a normal grayscale DQN on `CartPole` for 1000 training steps
  - `python main.py -g Acrobot-v1 -m DDQCNN_PCA` for training a convolutional PCA variant of a DDQN
  - `python main.py -g CartPole-v0 -a Random -e 1000` for a random policy